HHS Public Access

Author manuscript

Dev Biol. Author manuscript; available in PMC 2019 February 01.

Published in final edited form as:

Dev Biol. 2018 February 01; 434(1): 149–163. doi:10.1016/j.ydbio.2017.12.003.

Prdm13 is required for Ebf3+ amacrine cell formation in the retina

Noah B Goodson[a,b], **Jhenya Nahreini**[a,c], **Grace Randazzo**[a], **Ana Uruena**[d], **Jane E Johnson**[d], and **Joseph A Brzezinski IV**[a,*]

[a]University of Colorado Denver, Department of Ophthalmology

[b]University of Colorado Denver, Neuroscience Graduate Program

[d]University of Texas Southwestern Medical Center, Department of Neuroscience

Abstract

Amacrine interneurons play a critical role in the processing of visual signals within the retina. They are highly diverse, representing 30 or more distinct subtypes. Little is known about how amacrine subtypes acquire their unique gene expression and morphological features. We characterized the gene expression pattern of the zinc-finger transcription factor *Prdm13* in the mouse. Consistent with a developmental role, *Prdm13* was expressed by Ptf1a+ amacrine and horizontal precursors. Over time, Prdm13 expression diverged from the transiently expressed Ptf1a and marked just a subset of amacrine cells in the adult retina. While heterogeneous, we show that most of these Prdm13+ amacrine cells express the transcription factor Ebf3 and the calcium binding protein calretinin. Loss of *Prdm13* did not affect the number of amacrine cells formed during development. However, we observed a modest loss of amacrine cells and increased apoptosis that correlated with the onset timing of Ebf3 expression. Adult *Prdm13* loss-of-function mice had 25% fewer amacrine cells, altered calretinin expression, and a lack of Ebf3+ amacrines. Forcing *Prdm13* expression in retinal progenitor cells did not significantly increase amacrine cell formation, Ebf3 or calretinin expression, and appeared detrimental to the survival of photoreceptors. Our data show that *Prdm13* is not required for amacrine fate as a class, but is essential for the formation of Ebf3+ amacrine cell subtypes. Rather than driving subtype identity, Prdm13 may act by restricting competing fate programs to maintain identity and survival.

Graphical Abstract

*Author for correspondence: Joseph A. Brzezinski IV, University of Colorado Denver, Department of Ophthalmology, 12800 E. 19th Ave. Mail Stop 8311, RC1-North Room 5104, Aurora, CO 80016 303-724-6959. joseph.brzezinski@ucdenver.edu.
[c]Current address: Georgetown University School of Medicine.

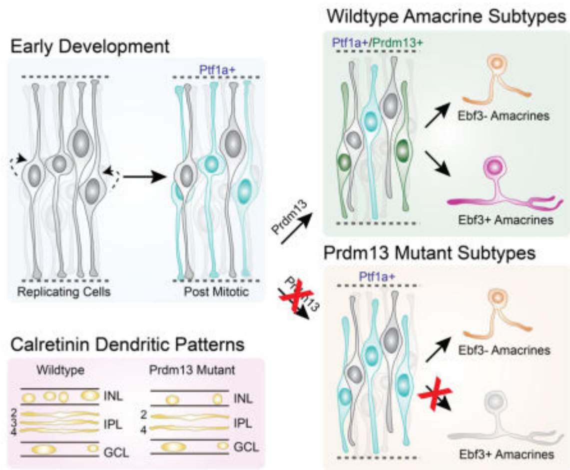

Keywords

Retinal development; Amacrine; Prdm13; Ebf3; Calretinin; Inner plexiform layer

INTRODUCTION

The retina is a thin neural tissue that detects and relays photic information. The mammalian retina has a highly organized structure consisting of alternating nuclear and synaptic (or plexiform) layers. These layers are populated by seven major classes of retinal neurons and glia, each of which are essential for normal vision. These cell types (rod and cone photoreceptors, Müller glia, retinal ganglion cell output neurons, and bipolar, horizontal, and amacrine cell interneurons) are all derived from a common progenitor population during development (Cepko, 2014; Turner and Cepko, 1987; Turner et al., 1990). Adding to the complexity of the system, most of the seven cell types can be further divided into more than 60 additional distinct subtypes (Euler et al., 2014; Masland, 2001; Sanes and Masland, 2015). While considerable progress has been made to uncover the transcription factors and signaling molecules that control major cell class development, relatively little is known about how subtypes acquire their identities.

Amacrine cells are primarily inhibitory interneurons. They form synapses with glutamatergic bipolar interneurons and ganglion cell output neurons in the inner plexiform layer (IPL). Their somas are predominantly located in the inner nuclear layer (INL), but a small fraction are displaced and localized to the ganglion cell layer (GCL). Amacrines make up only about 8% of retinal cells (Jeon et al., 1998), but within this population more than 30 distinct subtypes have been described (Badea and Nathans, 2004; MacNeil et al., 1999; MacNeil and Masland, 1998; Vaney, 1990). Amacrines can be grouped into three major categories based on whether they express GAD65/67 (GABAergic, ~43%), GlyT1 (glycinergic, ~43%), or neither of these markers (nGnG, ~15%) (Kay et al., 2011). The transcription factor Pax6 is made by all amacrines (de Melo et al., 2003), but subpopulations express a wide array of additional markers in a highly heterogeneous fashion. For example, subsets of amacrines are marked by transcription factors (*e.g.* AP2a, Ebf3, Bhlhb5), calcium binding proteins (*e.g.* calretinin, calbindin), and proteins involved in neurotransmission (*e.g.* ChAT, TH, vGlut3) (Bassett et al., 2007; Brecha et al., 1984; Feng et al., 2006; Haverkamp and Wassle, 2000, 2004; Huang et al., 2014; Johnson et al., 2004; Kay et al., 2011; Kondo et al., 1985). Many of these markers overlap in multiple subsets of amacrines, complicating the identification of individual subtypes. This has made interpreting the effects of gain- and loss-of-function experiments on amacrine cell development difficult.

In mice, progenitors that give rise to amacrine interneurons permanently exit the cell cycle (birthdate) from approximately embryonic (E) day 12.5 to postnatal (P) 2 (Cherry et al., 2009; Voinescu et al., 2009; Young, 1985). Progenitors that express the transcription factors Foxn4 and Rorb are competent to express Ptf1a (Fujitani et al., 2006; Li et al., 2004; Liu et al., 2013). Ptf1a is a basic-helix-loop-helix (bHLH) transcription factor that is transiently expressed in postmitotic cells that are restricted to forming amacrines and horizontal cells (Fujitani et al., 2006). Mice that lack *Ptf1a* die at birth and essentially lack horizontal and amacrine cells (Fujitani et al., 2006). Several transcription factors that are expressed by subsets of amacrine cells perturb subtype development when they are mutated. For example, *Isl1* mutants have reduced cholinergic (ChAT+) amacrines (Elshatory et al., 2007), loss of *Bhlhb5* decreases GABAergic subtypes (Feng et al., 2006), and *Neurod6* loss reduces nGnG (neither GABAergic nor glycinergic) amacrines (Kay et al., 2011). Birthdating experiments show that there is an overlapping genesis order for the major categories of amacrines, such that GABAergic cells are born early followed by glycinergic and nGnG amacrines (Cherry et al., 2009; Kay et al., 2011; Voinescu et al., 2009). While subtype choice is correlated with cell cycle exit timing, how and when postmitotic Ptf1a+ precursors commit to a specific amacrine subtype identity is unclear. Some perturbations, like *Neurod6* loss-of-function, alter subtype distribution without changing the total number of amacrines (Kay et al., 2011). This argues that fate choice is progressive, where Ptf1a+ cells first adopt amacrine identity before becoming further restricted to a particular subtype identity. To better understand the temporal and spatial mechanisms that diversify the Ptf1a+ precursor population, we looked for factors that act downstream of Ptf1a.

We have shown that the zinc finger transcription factor *Prdm13* is genetically downstream of *Ptf1a* in the spinal cord and retina (Chang et al., 2013). Within the spinal cord, Ptf1a directly activates *Prdm13*, which acts as a transcriptional repressor to promote inhibitory interneuron identity at the expense of excitatory fates (Chang et al., 2013). We have demonstrated that Prdm13 is recruited to enhancers by other transcription factors where it acts as a co-repressor (Mona et al., 2017). In particular, Prdm13 interacts with bHLH factors like Ptf1a in the developing spinal cord to convert transcriptional activators into repressors, helping to silence competing gene expression programs in bistable precursors (Mona et al., 2017). These data suggest that Prdm13 acts as a repressor in Ptf1a+ retinal cells to control amacrine or horizontal interneuron development.

We investigated the expression of Prdm13 during retinal development using specific antibodies and *Prdm13-GFP* knock-in mice. Consistent with our prediction, Prdm13 was expressed in Ptf1a+ amacrine and horizontal precursors throughout development. Prdm13 expression persisted into adulthood, primarily marking a heterogeneous subset of glycinergic and nGnG amacrines. The majority of Prdm13+ cells co-expressed calretinin and

Ebf3. Of note, the entire population of Ebf3+ amacrine cells co-expressed Prdm13. Mice that lacked *Prdm13* died at birth, but showed no deficits in amacrine cell genesis. To bypass lethality, *Prdm13-GFP* mice were bred to mice carrying a hypomorphic *Prdm13* allele (*Prdm13-Δ115*) (Mona et al., 2017). These compound heterozygous mice (*Prdm13-GFP/Δ115*) were viable and had fewer amacrine cells in the adult retina compared to control mice. In particular, these mice lacked Ebf3+ amacrines and calretinin+ cells that projected their dendrites to the middle of the IPL. Amacrine cell numbers were normal throughout their genesis period and declined only after the normal onset of Ebf3 expression in these mutants. Despite early widespread expression in Ptf1a+ cells, our data show that *Prdm13* is not required for amacrine cell genesis. However, *Prdm13* is required at a later step for amacrine subtype specification. *Prdm13* overexpression did not upregulate Ebf3 or calretinin, suggesting that *Prdm13* acts to suppress alternative gene regulatory networks to maintain Ebf3+ subtype identity and survival.

RESULTS

Prdm13 marks developing amacrine and horizontal cells

We previously showed that *Prdm13* is expressed by a subset of retinal cells that is similar to those marked by the committed amacrine and horizontal precursor marker *Ptf1a* (Chang et al., 2013; Fujitani et al., 2006). *Prdm13* in situ hybridization signal was lost in *Ptf1a* mutant embryos, suggesting that *Prdm13* is expressed by developing amacrine and horizontal cells. To better evaluate the spatial and temporal features of Prdm13 expression during retinal development, we immunostained retinal sections with antibodies against Prdm13 and Ptf1a. We focused on three time-points (E13.5, E15.5, and birth) when postmitotic nascent horizontals and amacrine cells co-express Ptf1a (Fujitani et al., 2006). We observed that both Prdm13 and Ptf1a immunostaining formed a mosaic pattern with oval nuclei located between the apical photoreceptor area and the ganglion cell layer (GCL) (Fig. 1). Prdm13 co-labeled 66.5% (± 21.3% SD) of Pft1a positive cells within the central and peripheral retina at E13.5 and all (100.0% ± 0.0% SD) of the Prdm13+ cells were Pft1a+ (Figs 1A–A‴, D). We observed similar numbers of Prdm13+, Ptf1a+, and double labeled cells at E15.5, but at this stage there was a statistically significant decrease in the percentage of Prdm13+ cells that co-expressed Ptf1a+ (89.8% ± 6.9% SD, N=7, t-test, $p<0.001$) (Figs 1B, D–E). P0 retinas had more Prdm13+ and Prdm13+/Ptf1a+ double labeled cells (Figs 1C, E). However, the percentage of Prdm13+ cells that co-expressed Ptf1a+ decreased further to 80.0% at P0 (Fig. 1D). This decreased percentage is consistent with the postnatal loss of Ptf1a expression (Fujitani et al., 2006) and the persistence of Prdm13 in a subset of postmitotic neurons. To determine whether Prdm13 was expressed in other cell types, we co-stained sections with Otx2, a marker of developing photoreceptors at these time-points (Beby and Lamonerie, 2013; Brzezinski and Reh, 2015; Fossat et al., 2007; Muranishi et al., 2011; Nishida et al., 2003). We observed modest overlap of Ptf1a, Prdm13, and Otx2 at all three time-points (Figs 1A–C, E). Since the *Ptf1a* lineage lacks photoreceptors (Fujitani et al., 2006), these double and triple labeled Otx2+ cells are already committed to becoming horizontals and/or amacrine cells. This plasticity in the Otx2+ lineage has been observed previously (Baas et al., 2000; Brzezinski et al., 2013; Das et al., 2009; Mills et al., 2017). We also co-labeled sections with antibodies against the ganglion cell marker Brn3 (Xiang et al., 1995). No

Prdm13+/Brn3+ ganglion cells were observed (data not shown). These data suggest that Prdm13 is expressed downstream of Ptf1a, marking only committed amacrine and/or horizontal cells.

Prdm13 null mice exhibit no gross changes in embryonic retinal development

We created a *Prdm13-GFP* knock-in mouse line to accurately and persistently label *Prdm13+* cells and conduct loss-of-function analysis (Mona et al., 2017). These mice were created by inserting a cytoplasmic GFP cassette followed by a stop codon into exon 1 of the *Prdm13* sequence (Fig. 2A–A′) (Mona et al., 2017). We observed that homozygous *GFP/GFP* null mice died at birth while *Prdm13* heterozygous animals showed no overt phenotypes (Mona et al., 2017). To track Prdm13 during retinal development, we examined *Prdm13-GFP* heterozygous and homozygous mice at E17.5 (Fig. 2), around the peak of amacrine cell genesis (Voinescu et al., 2009). The pattern of GFP immunostaining in both *GFP/+* and *GFP/GFP* mice at E17.5 mirrored that seen in wild-type (*+/+*) retinas labeled with anti-Prdm13 antibodies (Fig. 1 and data not shown). GFP labeled the cytoplasm, revealing apical and basal processes in both heterozygous and mutant animals (Fig. 2). Little if any staining was seen in the ganglion cell layer. There was appreciable basal clustering, with more staining in what will become the inner nuclear layer (Figs 2B–E). GFP intensity levels were lower in *GFP/+* mice compared to homozygous mutants, but the total number of GFP+ cells did not vary between the two populations (Fig. 2F) (N=6, t-test, p=0.9366), suggesting that *Prdm13* is neither required for its own expression nor to maintain cell survival at E17.5.

Next, we stained transgenic mice with antibodies against Prdm13 (Figs 2B–C). Prdm13 immunostaining overlapped highly with GFP in *Prdm13* heterozygous mice (Figs 2B, G). Some GFP+ cells in the nascent inner nuclear layer lacked Prdm13 staining. This population likely represents neurons that recently inactivated Prdm13 expression, but remained labeled due to the long half-life of GFP. Prdm13 immunostaining was completely absent from *Prdm13-GFP/GFP* null mice (Figs 2C, F–G), demonstrating the specificity of the antibody. The number of Prdm13+ cells was equivalent between *Prdm13* heterozygous and wild-type mice (N=6, t-test, p=0.8627) (Fig. 2G and data not shown).

To determine whether changes in cell fate occurred in *Prdm13* mutants, we examined E17.5 sections with antibodies against Otx2 to mark developing photoreceptors. The immunostaining pattern and intensity of Otx2+ nuclei was unchanged between *Prdm13* heterozygous and homozygous mutant retinas (Figs 2B–E). Consistent with our observations above (Fig. 1), a small number of Prdm13-GFP+ cells co-expressed Otx2 in both heterozygous and mutant animals (Figs 2B–E). Nonetheless, the number of these double labeled cells was unchanged between heterozygous and homozygous mice. This suggested that there was no change in photoreceptor genesis in *Prdm13* knockout animals. We then immunostained retinas with antibodies against Ptf1a to determine whether *Prdm13* affects the formation of horizontal and amacrine precursor cells (Figs 2D–E). The Ptf1a spatial labeling pattern was similar between *Prdm13* heterozygous and null animals (Figs 2D–E). The total number of Ptf1a+ cells was equivalent between wild-type, heterozygous, and *Prdm13* homozygous mutants (N=8, ANOVA, p=0.8131) (Fig. 2H). There were no differences in the number of Pft1a+/GFP+ cells between our lines (N=5, t-test, p=0.7193) or the fraction of Ptf1a+ cells that co-expressed GFP (N=5, t-test, p=0.3805) (Figs 2I–J). Similarly, we observed no differences in the number of cells that co-expressed Ptf1a and Otx2 between the three genotypes (N=8, ANOVA, p=0.2510) (Fig. 2K). These data argue that *Prdm13* is not required for the formation of amacrine and horizontal cell precursors. Though the number of Ptf1a cells was unaltered in mutants, the Ptf1a staining was typically more intense. This suggests that Prdm13 mediates a negative feedback loop onto *Ptf1a* in the retina, as has been observed in the spinal cord (Mona et al., 2017). Last, we examined retinas with antibodies against Brn3 to mark ganglion cells, but saw no differences in their numbers between genotypes (data not shown). Taken together, our data suggest that the loss of *Prdm13* does not alter the balance of cell fates formed during embryonic retinal development.

Prdm13 labels a subset of amacrine cells in the adult retina

Ptf1a is an early postmitotic marker for amacrine and horizontal cell precursors that is necessary for their development (Fujitani et al., 2006). Although Prdm13 initially overlaps with Ptf1a, as development progressed Prdm13+/Ptf1a negative cells became localized to the nascent inner nuclear layer. This suggested that Prdm13 expression remained in subsets of amacrine or horizontal cells. To test this, we immunostained mature (P30) *Prdm13 GFP/+* retinas for several amacrine and horizontal markers (Fig. 3). Nearly all of the GFP+ cell bodies were located in the inner aspect of the INL with cell processes extending into the inner plexiform layer (IPL). There were also a few GFP+ cell bodies within the GCL (Fig. 3). Immunostaining with Prdm13 antibodies overlapped with the GFP+ somas in heterozygous animals (data not shown). Prdm13 immunostaining was not as robust in adult animals, so we used GFP staining to better characterize the Prdm13+ population. Immunostaining for the pan-amacrine marker Pax6 revealed that 100.0% (± 0.0% SD) of GFP+ cells co-expressed Pax6+ (Fig. 3E and data not shown). However, only a subset of Pax6+ cells in the INL were GFP positive. These GFP+ cells accounted for 38.6% (± 2.9% SD) of all Pax6+ cells in the INL, suggesting that Prdm13 marks a subset of amacrine cells (Fig. 3F). No GFP+ cells co-expressed the photoreceptor and bipolar cell marker Otx2 (Fig. 3E) or the ganglion cell marker Brn3 (data not shown). We then immunostained retinas with markers that define subsets of amacrine and other interneuron populations in the retina. The transcription factor AP2a marks a large subpopulation of amacrine cells (Bassett et al., 2007). We observed that AP2a co-stained 31.3% (± 3.7% SD) of GFP+ cells (Figs. 3A, E). The transcription factor Bhlhb5 marks type II cone OFF bipolars and subsets of GABAergic and other amacrine cells (Feng et al., 2006; Huang et al., 2014). Bhlhb5 marked 34.9% (± 8.6% SD) of GFP+ cells (Figs 3A, D–E). In both cases, only subsets of AP2a+ (23.2% ± 3.5% SD) and Bhlhb5+ (27.1% ± 6.5% SD) cells co-expressed GFP (Fig. 3F and data not shown), reflecting the highly heterogeneous nature of amacrine cells and these markers. Calretinin and calbindin each mark complex subsets of amacrine cells in the mouse (Haverkamp and Wassle, 2000). Calretinin stains amacrine and ganglion cell somas in the INL and GCL, as well as three highly stereotypical dendritic sublaminae within the IPL (Haverkamp and Wassle, 2000; Lee et al., 2010). We observed that about half of Prdm13-GFP+ cells co-expressed calretinin (50.3% ± 9.2% SD) (Figs 3B, E). In contrast, GFP+ cells rarely co-expressed calbindin (0.6% ± 1.3% SD) and none of the intensely calbindin labeled horizontal cells (Peichl and Gonzalez-Soriano, 1994) made GFP (Figs 3B, E). Co-staining with the glycinergic marker GlyT1 (Menger et al., 1998; Pow and Hendrickson, 1999) and the GABAergic marker GAD65/67 (Haverkamp and Wassle, 2000) revealed that most of the Prdm13-GFP+ cells were glycinergic (Figs 3C, E). GlyT+ glycinergic amacrines accounted for 44.7% (± 9.2% SD) of GFP+ cells, while GABAergic GAD+ cells accounted for only 2.8% (± 2.4% SD) (Fig. 3E). These percentages may be underrepresented as not all amacrine somas were robustly labeled with these antibodies. Nonetheless, there is a clear preference for glycinergic overlap, consistent with the paucity of GFP+ displaced amacrine cells. We examined cholinergic amacrines by co-staining with Sox2 antibodies (Cherry et al., 2009; Surzenko et al., 2013; Taranova et al., 2006) (data not shown). We did not observe any overlap of GFP with Sox2 (Fig. 3E), showing that Prdm13 does not mark cholinergic amacrine cells. Similarly, we observed no overlap with vGlut3, which marks a small population of mostly glycinergic amacrines (Haverkamp and Wassle, 2004; Voinescu et al., 2009), or with the dopaminergic amacrine marker TH (Brecha et al., 1984) (data not shown). Lastly, we examined Prdm13-GFP/+ retinas with antibodies to Ebf3. Ebf3 marks glycinergic and nGnG amacrines along with subsets of ganglion cells (Jin et al., 2010; Kay et al., 2011). Many GFP+ cells co-expressed Ebf3 (70.4% ± 7.6% SD) (Figs 3D–E). To eliminate the possibility of counting Ebf3+ ganglion cells, we narrowed our quantification parameters to the Ebf3+ cells within the INL and found that 100% (± 0.0% SD) of them co-expressed GFP (Fig. 3F). This suggests that *Prdm13* marks the entire cohort of Ebf3+ amacrines, while also marking a smaller diverse set of non-Ebf3+ amacrine cells.

Ebf3+ amacrine cells are absent from *Prdm13* mutants

Many amacrine subtype differentiation markers appear postnatally. For example, Ebf3 expression in amacrine cells is first seen at P4 (Kay et al., 2011). To overcome the neonatal lethality of *Prdm13-GFP/GFP* null mice, we took advantage of a *Prdm13* allele with a 115bp deletion in the first exon (Fig. 4A) (Mona et al., 2017). This *Prdm13-Δ115* modification was predicted to result in a frame shift with early truncation of the Prdm13 protein (Fig. 4A). However, homozygous *Prdm13-Δ115* mice express some Prdm13 protein and were viable, suggesting that the 115bp deletion created a hypomorphic allele (Mona et al., 2017). We crossed the *Prdm13-GFP* mouse line with *Δ115* to create mice that had severely reduced *Prdm13* function. These *GFP/Δ115* mice were viable, and adults had a conspicuous loss of GFP+ cells (3.97 cells/100μm ± 1.07 SD) compared to *Prdm13-GFP/+* heterozygotes (16.06 cells/100μm ± 2.66 SD) (Figs 4B–C). The GFP+ cells remaining in *GFP/Δ115* mice were localized to the INL and generally had larger cell bodies compared to heterozygous control retinas (Fig. 4B). We next examined whether this loss of roughly 12 GFP+ cells/100μm was due to a reduction in amacrine cells or GFP expression. Pax6 immunostaining revealed no changes in the number of labeled cells in the GCL (N=6, t-test, p=0.299), but there was a significant decrease in Pax6+ INL cells from 39.68 (SD ± 3.24) cells/100μm in control mice to 31.11 (SD ± 5.71) cells/100μm in *GFP/Δ115* mice (N=6, t-test, p=0.028) (Fig. 4M and data not shown). This loss of Pax6 staining in the INL was similar in magnitude to the GFP reduction, suggesting that a subset of Prdm13+ amacrine cells were lost in *GFP/Δ115* mice. We then examined whether *Prdm13* perturbation affected specific amacrine subtypes. Immunostaining for GABAergic and glycinergic amacrines revealed no changes in the number of GAD+ cells, but a modest decrease in GlyT+ cells was observed in the *GFP/Δ115* mice (N=9, t-test, p=0.014) (Figs 4D–E, M). More conspicuous was the reduced number of GFP+ cells that co-expressed GlyT (N=9, t-test, p=<0.001) (Figs 4D–E, N). This suggested that the glycinergic amacrines that normally co-express Prdm13 were selectively reduced in mutants. We observed a slight increase in the number of GFP+ cells that co-expressed GAD65 in *GFP/Δ115* mice (N=9, t-test, p=0.014), but this modest change was not enough to alter the overall number of GABAergic amacrines in the retina (Figs 4D–E, M–N). The total number of AP2a and Bhlhb5+ amacrines was significantly reduced in *GFP/Δ115* mice compared to *GFP/+* controls (Figs 4F–G, M). The number of GFP+ cells that co-expressed AP2a or Bhlhb5 decreased proportionately in *GFP/Δ115* animals (Figs 4F–G, M–N). These data suggest that the Prdm13+ subpopulations of AP2a+ and Bhlhb5+ amacrines were specifically lost in mutants.

Prdm13 marked large fractions of calretinin and Ebf3 expressing amacrine cells in adult retinas (Fig. 3). As expected, calretinin staining was strikingly different between heterozygous control and *GFP/Δ115* mice (Figs 4H–I). There was a conspicuous loss of cell bodies and a change in the distribution of dendritic staining in the IPL (Figs 4H–I, L). Calretinin positive somas in the INL decreased from 13.47 (± 3.13 SD) cells/100μm in controls to 9.89 (± 1.52 SD) cells/100μm in the *GFP/Δ115* mice (N=9, t-test, p=0.0019) (Fig. 4M). There was nearly a total loss of GFP+/calretinin+ cells in the *GFP/Δ115* mice (N=9, t-test, p≪0.001) (Figs 4H–I, N). Calretinin strongly marks three (2, 3, and 4) of the five synaptic sublaminae of the IPL (Haverkamp and Wassle, 2000; Lee et al., 2010). Heterozygous control mice displayed this trilaminar calretinin pattern, while the *GFP/Δ115* mice had a thinner IPL that contained only two sublaminae (Figs 4H–I, L). The cholinergic amacrine marker ChAT, which labels sublaminae 2 and 4 (Haverkamp and Wassle, 2000; Voigt, 1986), was normal in *GFP/Δ115* mice (data not shown). There was a minor increase in the number of GFP+ cells that co-expressed calbindin in *GFP/Δ115* mice, but the IPL staining of sublaminae 2 and 4 (Haverkamp and Wassle, 2000) was normal (Figs 4H–I, M–N). These data argue that calretinin positive cells that project to sublamina 3 are lacking in *GFP/Δ115* mice (Fig. 4L). Since essentially all Ebf3+ amacrine cells co-expressed Prdm13, we expected this population to be the most disrupted in *GFP/Δ115* retinas. Indeed, we observed a nearly complete loss of Ebf3+ cells from the INL of these mutants (Figs 4J–K, M). This loss of about 10 Ebf3+ amacrine cells/100μm was nearly the same as the loss of Pax6+ INL cells in *GFP/Δ115* mice (Fig. 4M). Consistent with an amacrine cell-specific deficit, the number of Ebf3+ cells in the GCL was unchanged (N=9, t-test, p=0.26). The loss of both Ebf3+ and calretinin+ cells suggested that these populations overlap extensively. In adult wild-type mice, we observed that 72.2% (± 12.3% SD, N = 4) of calretinin+ cells in the INL co-expressed Ebf3+ and that 64.4% (± 7.0% SD, N = 4) of Ebf3+ cells in the INL were calretinin+ (Fig S1). Taken together, these data argue that *Prdm13* is required for the formation or survival of Ebf3+/calretinin+ cells.

Loss of the Prdm13+ amacrine population begins at P5

We did not observe a change in GFP+ cells in E17.5 *Prdm13* mutant mice (Fig. 2), but P30 *GFP/Δ115* mice had considerably fewer GFP+ cells and about ~25% fewer amacrines (Fig. 4). There are three general mechanisms that account for this reduction in cell numbers. These include: (1) a reduction in the number formed during development, (2) altered amacrine subtype fate choice, and (3) cell death. To distinguish between these possibilities, we examined mice at intermediate developmental time-points (Fig. 5). We stained E17.5 *GFP/+* and *GFP/GFP* mice for Pax6 and observed no significant differences in cell number (N=4, t-test, p=0.62) (Figs 5A–B). Next, we compared the number of intensely Pax6+ INL cells between *GFP/+* and *GFP/Δ115* retinas at P2, the end of amacrine cell genesis. We observed no statistically significant differences (N=2, t-test, p=0.98) between the genotypes, arguing that amacrine fate specification as a class was unaltered by the loss of *Prdm13* (Figs 5C–D).

Many amacrine subtype-specific markers become expressed in the first postnatal week, including Ebf3 starting at P4 (Kay et al., 2011). We next examined P5 GFP/+ control and *GFP/Δ115* mutant retinas for the numbers of GFP, Ebf3, and Bhlhb5 positive amacrine cells. At P5, nascent IPL lamination was less delineated and thinner in *GFP/Δ115* retinas (Figs 5E–F). Nonetheless, we observed only a modest decrease (N=7, t-test, p=0.027) in the number of GFP+ cells in mutant retinas compared to heterozygous controls (Figs 5E–F, I). Ebf3 staining was strongly reduced in the INL of *GFP/Δ115* mice, but was abundant in the GCL of both controls and mutants (Figs 5E–F). Both control and mutant Ebf3+ cells in the INL co-expressed GFP, but there were far fewer Ebf3+ nuclei in *GFP/Δ115* retinas (Figs 5E–I). The near absence of Ebf3+ amacrines in adult mice is also seen at P5, suggesting that Ebf3+ cells are not formed in *GFP/Δ115* mice. While the overall number of Bhlhb5+ amacrines did not change significantly, more of these cells co-expressed GFP in P5 mutants compared to controls (Figs 5E–I). This change suggests that some of the Prdm13-GFP+ cells that would have adopted Ebf3+ subtype identity failed to do so and instead express Bhlhb5 and perhaps other subtype markers. This is further supported by the modest loss of P5 GFP+ cells compared to adult *GFP/Δ115* retinas. We reasoned that inappropriately specified cells may undergo apoptosis. Staining for activated caspase 3 (AC3) at P5 revealed no appreciable overlap with GFP in control mice, but 28.1% of dying AC3+ cells co-expressed GFP+ in *GFP/Δ115* mutants (N=4, t-test, p=0.029) (Fig. 5J and data not shown). These data suggest that *Prdm13* is required for Ebf3+ amacrine subtype formation and survival.

Prdm13 overexpression is not sufficient to drive ectopic amacrine formation

We observed that *Prdm13* is not required for amacrine cell generation as a class. Nonetheless, it could play a redundant role in amacrine genesis and an instructive role in subtype formation. We hypothesized that ectopic expression of *Prdm13* would promote amacrine formation, and in particular, subtypes that express Ebf3 and/or calretinin. To test this, we created plasmid expression vectors to drive *Prdm13* (WT), which has been shown to act as a transcriptional repressor (Chang et al., 2013; Mona et al., 2017). We also created a vector to express a *VP16* fusion with *Prdm13* (VP16) (Chang et al., 2013) to convert it into a transcriptional activator. Each of these vectors contains the *Ef1α* enhancer to drive ubiquitous expression and an *IRES-Cre* cassette for indirect detection. As a control, we used an *Ef1α* driven nuclear cherry plasmid (Wilken et al., 2015). Constructs were electroporated into newborn retinas and cultured for 2 or 7 days *in vitro* (DIV) as intact explants. Electroporation preferentially affects retinal progenitor cells, which give rise to photoreceptors and to a lesser extent bipolars, glia, and amacrine cells at this stage (Turner and Cepko, 1987; Young, 1985). Electroporated explants were stained for Pax6 and Otx2

(Fig. 6) as they mark all cell types (Otx2- photoreceptors and bipolars, Pax6- horizontals, amacrines, glia, and ganglion cells) in the mature retina. At both 2DIV and 7DIV, control cherry cells detected with anti-red fluorescent protein (RFP) antibodies were overwhelmingly Otx2+ photoreceptors and bipolar cells, consistent with the fate distribution of newborn progenitors (Turner and Cepko, 1987) (Figs 6A, D). Only about 20% of electroporated control cells made Pax6, indicative of an amacrine or glial identity (Figs 6A, E). In contrast to cherry controls, both Prdm13 WT and VP16 electroporated cells were localized to the nascent INL and were much more likely to co-express Pax6 (N = 26, ANOVA, P=0.0003) than Otx2 at 2 DIV (Figs 6A–E). At 2DIV, both WT and VP16 had significantly fewer Otx2+ cells and significantly more Pax6+ cells than cherry control. At 7DIV the overall pattern was similar, such that Prdm13 WT and VP16 transfected cells co-expressed Pax6 more frequently than cherry controls (N=24, ANOVA, 0.0111) (Figs 6D–E). However, it was apparent at 7DIV that many Prdm13-VP16 transfected cells co-expressed both Otx2 and Pax6 (Figs 6C, D–F). The co-expression of Otx2 and Pax6 was seldom observed in cherry control or Prdm13 WT transfections (Fig. 6F). Some retinal progenitors appear to transiently co-express Pax6 and Otx2 (Brzezinski et al., 2010; Muranishi et al., 2011), raising the possibility that VP16 cells remain as undifferentiated progenitors. Alternatively, the VP16 fusion may lead to the inappropriate activation of photoreceptor genes, like *Otx2*. Prdm13 WT transfected cells differed from VP16 and control cells in another way. Many Prdm13 WT transfected cells failed to express either Pax6 or Otx2 (Fig. 6B–B‴, inset). These non-Pax6 non-Otx2 cells of unknown identity accounted for nearly 30% of Prdm13 WT transfected cells at 7DIV (Figs 6B–B‴, data not show). Non-Pax6, non-Otx2 electroporated cells were absent from 7DIV Cherry control and Prdm13 VP16 transfections.

The presence of Otx2+/Pax6+ cells in VP16 electroporations and the non-Pax6 non-Otx2 cells in Prdm13 WT conditions raised the possibility that these constructs were deleterious to cell survival. Accordingly, both Prdm13 WT and VP16 fusion transfections resulted in sparse numbers of Cre+ electroporated cells at both 2DIV and 7DIV compared to cherry control transfections (Figs 6B–F and data not shown). We observed this reduction at 1, 3, 4, and 10DIV as well (data not shown). Moreover, our initial electroporation experiments with higher concentrations of Prdm13 WT and VP16 plasmids resulted in even fewer Cre+ cells after only 1DIV (data not shown). These findings suggested that overexpression of Prdm13 WT and VP16 conferred an immediate survival disadvantage to transfected cells. The bias towards Pax6 expression and INL localization suggested that both Prdm13 WT and VP16 were especially toxic to Otx2+ photoreceptors and bipolar cells. We also searched for upregulation of Ebf3, calretinin, calbindin, and Bhlhb5 at 2, 3, 4, and 7DIV. However, we did not observe any ectopic expression of amacrine markers at these time-points (data not shown). Taken together, our data suggest that *Prdm13* is not sufficient to drive ectopic amacrine cell formation in the newborn retina. Instead, *Prdm13* appears to be toxic to nascent photoreceptors.

DISCUSSION

How the developing retina allocates a set number of amacrine cells and diversifies them into 30+ subtypes is only partially understood. We investigated the transcription factor *Prdm13* and found that it was expressed broadly in developing amacrine cell precursors and became restricted to a heterogeneous subset of amacrines in mature mice. Normal numbers of amacrine cells formed in *Prdm13* mutant mice, but subtype specification was altered in the early postnatal period. Ebf3+ amacrine cells were absent and about 25% of amacrine cells were subsequently lost to cell death. Our data show that *Prdm13* does not control amacrine cell genesis as a class, but is instead necessary for subtype fate choice and cell survival. Future work is needed to uncover how *Prdm13* regulates the formation of Ebf3+ amacrines and how individual subtypes within this heterogeneous population function in the retina.

***Prdm13* is not necessary for amacrine identity**

We observed that *Ptf1a* mutant retinas lack *Prdm13* expression (Chang et al., 2013). Therefore, we expected Prdm13 to function downstream of Ptf1a in the developing retina. Consistent with this model, 100% of Prdm13+ cells co-expressed Ptf1a at E13.5. In the spinal cord, Ptf1a drives *Prdm13* expression, which then feeds back to inhibit *Ptf1a* expression (Hanotel et al., 2014; Mona et al., 2017). This negative feedback loop is also present in the retina since *Prdm13* mutant mice had more intensely stained Ptf1a+ cells. Despite this expression increase, *Prdm13* loss did not change the number of Ptf1a+ cells in the retina or the number of amacrine cells that were initially formed. This suggests that feedback is important for controlling *Prdm13* levels and in turn, amacrine subtype fate choice and survival (see below). Despite Prdm13 being expressed at early stages in Ptf1a+ cells, it was not required for the formation of amacrine or horizontal cell precursors.

Since *Prdm13* acts as a repressor, we reasoned that it acts by blocking competing cell identities in multipotent precursors (Chang et al., 2013; Mona et al., 2017). This was reinforced by our observation that some Ptf1a+ and Prdm13+ cells transiently co-expressed Otx2. This overlap is consistent with data suggesting that Otx2+ cells can adopt amacrine and horizontal cell identities (Baas et al., 2000; Brzezinski et al., 2013; Das et al., 2009; Mills et al., 2017). It has been shown that the Ptf1a+ lineage contains only horizontal and amacrine cells (Fujitani et al., 2006). We hypothesized that Prdm13 represses *Otx2* expression in Ptf1a+ cells to restrict fate choice. However, we did not observe an increase in Otx2+ cells in *Prdm13* mutants or a fate shift to photoreceptors or bipolar cells. This shows that *Prdm13* is not required to suppress photoreceptor identity in Ptf1a+ cells. Interestingly, Prdm13-VP16 activator misexpression increased the number of Pax6+ cells that co-expressed Otx2. This raises the possibility that Prdm13 normally inhibits *Otx2* expression in the developing retina. For this to be true, other factors must compensate for or act redundantly with *Prdm13* to suppress *Otx2* expression. Since *Ptf1a* misexpression can promote amacrine identity at the expense of photoreceptors and bipolar cells (Jin et al., 2015; Watanabe et al., 2015), fate restriction appears to be downstream of Ptf1a. The transcription factors AP2a (*Tfap2a*) and AP2b (*Tfap2b*) are both decreased in *Ptf1a* mutants (Jin et al., 2015). Gain-of-function analysis showed that these factors can promote amacrine formation (Jin et al., 2015). However, deletion of both genes simultaneously resulted in only a modest amacrine phenotype and there was no appreciable fate shift to Otx2+ photoreceptors or bipolar cells (Bassett et al., 2012). It remains unclear how Ptf1a+ cells are restricted to horizontal and amacrine cell fates and whether *Prdm13* plays a redundant role in this process.

Prdm13 marks multiple subtypes of amacrine cells

Amacrine cells are highly diverse, with estimates of 30 or more discrete subtypes in the mouse retina. About one third of amacrine cells were marked by Prdm13 in the adult retina. Prdm13 labeled a heterogeneous group of glycinergic and nGnG amacrines, but did not mark cholinergic, dopaminergic, or glutamatergic amacrine subtypes. Recent reports have also shown that Prdm13 is made by subsets of amacrine cells. In mice and frogs, most Prdm13+ cells are glycinergic (Bessodes et al., 2017; Watanabe et al., 2015). The frog retina has more Prdm13+ cells that are GABAergic compared to mice (Bessodes et al., 2017; Watanabe et al., 2015). Our characterization of subtype markers is similar to those described previously in mice (Watanabe et al., 2015), except that we observed far fewer Prdm13+ cells that co-expressed calbindin or GAD65. The reason for these discrepancies is unclear, but may involve differential sensitivities of antibodies used in each study. We examined additional subtype markers, including Bhlhb5 and Ebf3, to further probe the diversity of Prdm13+ amacrine cells. Strikingly, we found that Ebf3+ cells are the only amacrine population that is entirely Prdm13 labeled.

Our experiments revealed that nearly 75% of Prdm13+ amacrine cells co-expressed Ebf3. The Ebf3+ population is itself heterogeneous, representing a 3-to-1 mix of glycinergic and Neurod6+ nGnG subtypes (Kay et al., 2011). The glycinergic subpopulation has narrow, multistratified dendritic fields that project to sublaminae 1–4 in the IPL (Kay et al., 2011). The nGnG Ebf3+ population has similar morphology, but projects dendrites to sublaminae 1–3 (Kay et al., 2011). We observed a small number of Ebf3+ amacrines that co-expressed Bhlhb5, raising the possibility that Ebf3+ amacrines can be divided into additional subtype groups. This is supported by single cell profiling experiments that identified three Ebf3+ clusters (one glycinergic and two nGnG) in the retina (Macosko et al., 2015). About one fourth of the Prdm13+ amacrines did not co-express Ebf3. There was no conspicuous marker that labeled all of these cells, suggesting they are a heterogeneous population. This likely includes the small number of GABAergic amacrines, the bulk of the Bhlhb5+ subtypes, and additional glycinergic and nGnG amacrines. Going forward, intersecting Prdm13 with other subpopulation markers may uniquely define individual amacrine subtypes and facilitate experiments to uncover their physiology.

Prdm13 affects amacrine subtype specification

Despite expression at early time-points in Ptf1a+ cells, *Prdm13* mutants had no discernable phenotypes embryonically. In fact, there were no conspicuous changes in *Prdm13* loss-of-function mice until P5. This is after the timing of amacrine cell birth, but overlaps with subtype maturation and culling of excess generated amacrines (Cherry et al., 2009; Kay et al., 2011; Pequignot et al., 2003; Strettoi and Volpini, 2002; Voinescu et al., 2009; Voyvodic et al., 1995; Young, 1984, 1985). At P5, *Prdm13-GFP/Δ115* mice showed increased apoptosis and largely lacked Ebf3+ amacrines. GFP+ cells in these mice were more likely to co-express Bhlhb5 than controls, suggesting that subtype specification was altered. This supports a model where *Prdm13* is required for Ebf3+ amacrine subtype specification. By the adult stage *Prdm13-GFP/Δ115* mice have fewer amacrines and essentially lack Ebf3+ subtypes. This argues that *Prdm13* is also required for the survival of Ebf3+ amacrine cells. It is difficult to determine whether *Prdm13* controls amacrine subtype specification, survival, or both. One possibility is that Ebf3+ amacrines are still specified in mutants, but die without *Prdm13* due to derepression of genes made by other subtypes. Another possibility is that Ebf3+ amacrines fail to become specified in mutants. This is consistent with our observations of a significant reduction of Ebf3 expression that precedes cell death. In the absence of subtype specification, cells could die due to a lack of identity or they could adopt a different subtype choice. Though calbindin+ amacrines increased subtly in mutants, most amacrine types profiled (including Bhlhb5+ cells) decreased modestly. This argues against a fate shift; however, upwards of 50% of amacrines are normally culled during the early postnatal period (Pequignot et al., 2003; Strettoi and Volpini, 2002; Voyvodic et al., 1995; Young, 1984). Thus, an excess of improperly specified amacrine subtypes could be masked by apoptosis. In the frog, *Prdm13* morpholinos reduced glycinergic amacrines without increasing GABAergic numbers (Bessodes et al., 2017). Similarly, Watanabe and colleagues observed a reduction of glycinergic amacrines without an increase in other subtypes in *Prdm13* mutant mice carrying a distinct allele to those used here (Watanabe et al., 2015). Taken together, these loss-of-function data are consistent with roles for *Prdm13* in both subtype specification and survival.

Gain-of-function experiments suggest a more active role for *Prdm13* in fate choice. Overexpression of *Prdm13* in the frog retina biased cells towards glycinergic amacrine fate at the expense of bipolar cells and glia (Bessodes et al., 2017). Watanabe and colleagues overexpressed *Prdm13* in newborn mice and observed that most transfected cells adopted amacrine fate (Watanabe et al., 2015). Moreover, *Prdm13* overexpression modestly increased the fraction of transfected cells that expressed calretinin and/or calbindin (Watanabe et al., 2015). These findings argue that *Prdm13* is sufficient to specify amacrine type and subtype identity. Based on these findings, we expected *Prdm13* overexpression to drive ectopic Ebf3+/calretinin+ amacrine cell formation. Though we observed that *Prdm13* overexpressing cells were more likely to make Pax6, they did not ectopically express Ebf3 or calretinin. Thus, *Prdm13* is not sufficient to instruct Ebf3+ amacrine subtype formation. We also observed a strong reduction in the number of Prdm13 transfected cells compared to control. Many transfected cells failed to express Otx2 or Pax6, which mark progenitors and specified retinal cells. These double negative cells are likely poised for apoptosis. Our data suggest that *Prdm13* overexpression is especially toxic to developing photoreceptors and to a lesser extent, progenitors and other cell types. Thus, we may be observing selection instead of fate changes in these gain-of-function experiments. Overexpressing Prdm13-VP16 also appeared toxic in the retina. This toxicity is likely caused by a different mechanism because Prdm13-VP16 increased the fraction of cells that co-expressed Otx2 and Pax6. This forced activator activity may upregulate competing gene regulatory networks and cause apoptosis. Due to the toxicity we observed, future experiments where *Prdm13* is specifically overexpressed in postmitotic amacrine cell precursors will reveal whether it instructs Ebf3+ subtype identity.

North Carolina Macular Dystrophy (OMIM-136550) has been attributed to dominantly inherited mutations in *PRDM13* (Small et al., 2016). This includes duplication of the coding sequence and non-coding point mutations flanking *PRDM13* (Bowne et al., 2016; Manes et al., 2017; Small et al., 2016). This disorder is developmental in nature and affects the structure of the macula, resulting in a highly variable loss of photoreceptors and central vision. It is unlikely that this represents haploinsufficiency, as *Prdm13* heterozygous mice have no overt deficits in development. Instead, the pathology is consistent with a *PRDM13* gain-of-function. Since Prdm13 is expressed in Ptf1a+ committed amacrine and horizontal cell precursors, it seems unlikely that increased *PRDM13* dosage would negatively affect photoreceptor formation. Instead, mutations that drive ectopic *PRDM13* expression in progenitors or nascent photoreceptors could either bias their fate towards amacrine cell identity or cause toxicity. One of these non-coding mutations (V2) (Small et al., 2016) creates a potential *Otx2* binding site (Bunt et al., 2011), which may create a photoreceptor-specific enhancer for *PRDM13*. Our initial attempts to examine whether the non-coding mutations create novel retinal enhancers in developing mice were unsuccessful. Though our experiments suggest that *Prdm13* kills nascent photoreceptors, other experiments did not note toxicity (Bessodes et al., 2017; Watanabe et al., 2015). Due to the heterogeneity of mutations and the disease severity, it seems likely that more than one mechanism underlies the pathophysiology of North Carolina Macular Dystrophy.

Function of Ebf3+ amacrine cells in the retina

We and others observed a decrease in the number of calretinin+ amacrines in *Prdm13* mutants (Watanabe et al., 2015). Interestingly, calretinin staining of the IPL was altered such that the prominent sublamina 3 band was absent. This suggests that calretinin+ dendrites that project to sublamina 3 are absent or re-routed. We observed that many Ebf3+ amacrine cells co-expressed calretinin (~62%). Since Ebf3+ cells are essentially absent in *Prdm13* mutants, we reasoned that Ebf3+/calretinin+ cells normally project dendrites to sublamina 3 of the IPL. Kay and colleagues showed that Ebf3+ glycinergic amacrines (75%) projected to sublaminae 1–4, whereas Ebf3+ nGnG amacrines (25%) have dendrites in sublaminae 1–3 (Kay et al., 2011). Overexpression of *Neurod6* increased the nGnG fraction of amacrines, creating prominent dendritic bands in sublaminae 1 and 3 of the IPL (Kay et al., 2011). Thus, the loss of Ebf3+ nGnG amacrines in *Prdm13* mutants may explain the loss of calretinin labeling of sublamina 3. Alternatively, calretinin+ cells that do not co-express Ebf3 and project to sublamina 3 may be lost or misrouted. Lastly, it is possible that loss of Ebf3+ and other amacrine subtypes in *Prdm13* mutants has a non-autonomous effect on the localization of calretinin+ dendrites.

The profound loss of Ebf3+ amacrines and disruption of the IPL should alter the normal physiology of the retina. The complex nature of the cells lost and limited knowledge of amacrine physiology make this difficult to study. Watanabe and colleagues showed that scotopic and photopic electroretinography was normal in *Prdm13* mutants (Watanabe et al., 2015). They also examined optokinetic reflex response behaviors. Interestingly, these behavioral tests showed that *Prdm13* mutant mice had greater spatial and contrast sensitivity than control mice (Watanabe et al., 2015). Since Ebf3+ amacrines are most disrupted in *Prdm13* mutants, the loss of these amacrines likely caused the observed sensitivity increases, ostensibly at the expense of other visual functions (Bowrey and James, 2015; Sugita et al., 2015). A more narrow dissection of the amacrines disrupted in *Prdm13* mutants is needed to determine how defined amacrine subtype(s) contribute to visual behaviors.

METHODS

Mice

Mice were used in accordance with procedures approved by the local IACUCs at the University of Colorado Denver and the University of Texas Southwestern Medical Center (UTSW). Wild-type mice, *C57BL/6J*, were obtained from The Jackson Labs (Bar Harbor, ME). *Prdm13* gene targeted mouse lines were created at UTSW (Mona et al., 2017). Briefly, *Prdm13-GFP* (*GFP/GFP)* mice were developed using zinc-finger nuclease targeting technology such that a GFP cassette followed by a stop codon was inserted into the first exon of *Prdm13* (Fig. 2A). Homozygous mutant mice died at or before birth. Mice were genotyped by PCR at 60°C annealing with three primers: 5′-GCTGCTCCTGGTTCTGTCA-3′, 5′-CCTTTTCTCTGCTGCTCGTC-3′ and 5′-GCTGGAGTACAACTACAACAGCCA-3′ to generate 313bp wild-type and 549bp mutant bands (Mona et al., 2017). A presumed hypomorphic allele of *Prdm13* (Δ115) was the result of creating a 115bp deletion within the first exon of *Prdm13* (Fig. 4A′) (Mona et al., 2017). While this deletion was predicted to create a null allele, homozygous *Δ115/Δ115* mice live to adulthood and express Prdm13 protein in the developing neural tube (Mona et al., 2017). The features of the two *Prdm13* alleles used here and those of two additional mutant lines are described in detail by Mona and colleagues (Mona et al., 2017). PCR genotyping was done at 60°C annealing with two primers: 5′-GCTGCTCCTGGTTCTGTCA-3′ and 5′-CCTTTTCTCTGCTGCTCGTC-3′ to yield 313bp wild-type and 198bp mutant bands (Mona et al., 2017).

Plasmid creation

A *Prdm13* expression plasmid was made by inserting the wild type mouse *Prdm13* cDNA sequence under the control of a ubiquitous human Ef1α enhancer, followed by IRES2 sequence and cDNA for Cre recombinase and a β-globin polyadenylation sequence. The *Prdm13-VP16* construct was cloned similarly, but used a previously constructed C-terminal VP16 fusion protein sequence (Chang et al., 2013). Both constructs were validated by Sanger sequencing and Cre immunostaining of transfected explants (data not shown). We used a plasmid containing an Ef1α enhancer driving nuclear localized cherry fluorescent protein as an electroporation control (Wilken et al., 2015).

Dissection, electroporation, and culturing

Newborn eyes were collected immediately after animals were sacrificed. The eyes were extracted with forceps, dissected in cold HBSS+ (HBSS, Ca2+, Mg2+, 6 mg/mL glucose, and 0.05M HEPES), and transferred to calcium and magnesium free phosphate buffer solution (PBS) for electroporation (Mills et al., 2017). Retinas were oriented with the photoreceptor side up and 1μL of 2μg/μL DNA in 30% glycerol with methyl green was pipetted onto their surface. They were then electroporated with five 50ms square-wave pulses of 50mV at 125ms intervals from a BioRad Gene Pulser Xcell (BioRad, Hercules, CA, USA). Retinas were cultured in Neurobasal media, with 1X N2 supplement, 1X L-glutamine, 1X penicillin/streptomycin, and 1% FBS (Gibco/ThermoFisher Scientific, Waltham, MA, USA) (Mills et al., 2017). For 1 DIV cultures, retinas were placed in 12 well plates floating in 1mL of media. For all other cultures, retinas were flat mounted with their photoreceptor surface facing up on 0.4μm Milicell CM cell culture inserts (Milipore, Billerica, MA, USA) in 6 well plates with 1mL of media in the well, such that retinas were maintained at the air-media interface. Half the media was changed every other day. All cultures were kept at 37°C and 5% CO_2.

Prdm13 antibodies and immunohistochemistry

Three different rabbit antibodies against PRDM13 were generated in the Johnson lab at UTSW: PRDM13-Ab1 (ZF) PA6658, PRDM13-Ab1 (ZF) PA6659, and PRDM13-Ab2 (FL) TX970 (Mona et al., 2017). The antigens were bacterially expressed C-terminal domain of PRDM13 including amino acids 622 to 755 (ZF) or full length protein (FL), respectively. PA6658, PA6659, and TX970 were validated by western blot and tested on embryonic retinas. All three antibodies showed an equivalent expression pattern, but preparation PA6658 was the most robust reagent. To validate the specificity of the antibody, we immunostained (see below) E17.5 *Prdm13-GFP/GFP* null animals with the PA6658 antiserum and observed a total loss of signal compared to equivalently stained heterozygous E17.5 retinas (Fig 2).

Tissues for immunohistochemistry (IHC) were fixed in 2% paraformaldehyde for 1–2 hours at room temperature. Samples were cryoprotected at 4°C with an increasing concentration series (10–30%) of sucrose solutions in PBS, and flash frozen in OCT (Sakura Finetech, Torrance, CA, USA). Retinas and whole eyes were cryosectioned at 10um and transferred to Shandon Colorfrost Plus microscope slides (ThermoFisher Scientific, Waltham, MA, USA).

All IHC procedures were conducted as previously described (Brzezinski et al., 2010; Brzezinski et al., 2013; Mills et al., 2017; Park et al., 2017). Briefly, slides were washed in PBS, blocked with 5% milk block (the supernatant of a solution of 5% powdered milk, 0.5% TX100, 0.2% NaN_3, in PBS) for two hours, PBS washed, and placed with primary antibody in 5% milk block overnight at room temperature. After 18–24 hours, slides were washed in PBS, and treated with secondary antibodies in 5% milk block for 2 hours in the dark. Slides were given a final PBS wash, and covered with either Fluoromount-G (eBioscience Inc, San Diego, CA, USA) or Fluoro-Gel II with DAPI (Electron Microscopy Science, Hatfield, PA, USA).

The following primary antibodies were used at the given concentrations: mouse anti-AP2α (1:400; 5E4-c, DSHB Iowa City, Iowa USA); goat anti-Bhlhb5 (1:500; sc-6045, Santa Cruz Biotechnology, Inc, Santa Cruz, CA, USA); mouse anti-Brn3a (1:500; sc-6026, Santa Cruz Biotechnology, Inc); rabbit anti-Calbindin (1:400; AB1778, Millipore, Temecula, CA, USA); mouse anti-Calretinin (1:500; MAB1568. Millipore); rabbit anti-ChAT (1:400; AB143, Millipore); sheep anti-Chx10 (1:400; X1179P, Exalpha Biologicals Inc, Shirley, MA, USA); mouse anti-Cre (1:250; MAB3120, Millipore); mouse anti-Ebf3 (1:400; H00253738-M05, Abnova, Taipei, Taiwan); rabbit anti-Gad65/67 (1:400; AB1511, Millipore); mouse anti-GFP (1:1000; ab13970, Abcam Inc, Cambridge, MA, USA); goat anti-GlyT (1:500; AB1770, Millipore); mouse anti-Lhx1 (1:400; 4F2-c, DSHB); goat anti-Otx2 (1:250; AF1979, Bio-Techne Corporation, Minneapolis, MN, USA); rabbit anti-Pax6 (1:500; PRB-278P, Covance, Princeton, NJ, USA); guinea pig anti-Ptf1a (Hori et al., 2008); rabbit anti-Prdm13 (see above) (1:250); rabbit anti-recoverin (1:500; AB5585, Abcam Inc);

mouse anti-RFP (1:1000; ab65856, Abcam Inc); goat anti-Sox2 (1:500; sc-17320, Santa Cruz Biotechnology Inc); rabbit anti-tyrosine hydroxylase (TH) (1:100, ab152, Milipore); rabbit anti-vGlut3 (1:100; Cat# 135 203, Synaptic Systems, Göttingen, Germany).

All images were captured using an either an Olympus FV1000 laser scanning confocal microscope (Waltham, MA, USA) or a Nikon C2 laser scanning confocal microscope (Melville, NY, USA). The images were minimally processed using both ImageJ (Schneider 2012) and Adobe Photoshop CS5 (San Diego, CA, USA).

Cell Counts and Statistics

Images were taken from both eyes in male and female mice and include central and peripheral retinal areas. Images were viewed in Adobe Photoshop and cells were quantified manually. In about half of the cases, image quantification was repeated by a different co-author to improve accuracy. For each particular stain, retinas were imaged in 2–4 locations and the counts pooled to calculate the mean and standard deviation (SD). For plots, the error bars represent the SD. In most cases, two-tailed unpaired t-tests with the assumption of heteroscedasticity were utilized for statistical comparisons, and the degrees of freedom are based on the number (N) of mice examined or the number (N) of retinas electroporated. For multiple comparisons, 1 way ANOVA was used. In all cases, a $p<0.05$ was considered significant. Analyses were performed using Microsoft Excel (Microsoft, USA).

Supplementary Material

Refer to Web version on PubMed Central for supplementary material.

Acknowledgments

The authors thank Erin Kibodeaux, Trisha Savage, Rahul Kollipara, Joshua Chang, Joseph Adewumi, Ko Park, Jason Silver, Michael Kaufman, Michael Schwanke, Stephanie Bersie, Tom Reh, and Akina Hoshino for advice, technical support, and reagents. Experiments were supported in part by R01-HD037932 and R37-HD091856 to JEJ, and R01-EY024272 to JAB and by a Challenge Grant to the Department of Ophthalmology from Research to Prevent Blindness, Inc. JAB was supported in part by the Boettcher Foundation.

References

Baas D, Bumsted KM, Martinez JA, Vaccarino FM, Wikler KC, Barnstable CJ. The subcellular localization of Otx2 is cell-type specific and developmentally regulated in the mouse retina. Brain Res Mol Brain Res. 2000; 78:26–37. [PubMed: 10891582]

Badea TC, Nathans J. Quantitative analysis of neuronal morphologies in the mouse retina visualized by using a genetically directed reporter. J Comp Neurol. 2004; 480:331–351. [PubMed: 15558785]

Bassett EA, Korol A, Deschamps PA, Buettner R, Wallace VA, Williams T, West-Mays JA. Overlapping expression patterns and redundant roles for AP-2 transcription factors in the developing mammalian retina. Dev Dyn. 2012; 241:814–829. [PubMed: 22411557]

Bassett EA, Pontoriero GF, Feng W, Marquardt T, Fini ME, Williams T, West-Mays JA. Conditional deletion of activating protein 2alpha (AP-2alpha) in the developing retina demonstrates non-cell-autonomous roles for AP-2alpha in optic cup development. Mol Cell Biol. 2007; 27:7497–7510. [PubMed: 17724084]

Beby F, Lamonerie T. The homeobox gene Otx2 in development and disease. Exp Eye Res. 2013; 111:9–16. [PubMed: 23523800]

Bessodes N, Parain K, Bronchain O, Bellefroid EJ, Perron M. Prdm13 forms a feedback loop with Ptf1a and is required for glycinergic amacrine cell genesis in the Xenopus Retina. Neural Dev. 2017; 12:16. [PubMed: 28863786]

Bowne SJ, Sullivan LS, Wheaton DK, Locke KG, Jones KD, Koboldt DC, Fulton RS, Wilson RK, Blanton SH, Birch DG, Daiger SP. North Carolina macular dystrophy (MCDR1) caused by a novel tandem duplication of the PRDM13 gene. Mol Vis. 2016; 22:1239–1247. [PubMed: 27777503]

Bowrey HE, James MH. Commentary: "Prdm13 regulates subtype specification of retinal amacrine interneurons and modulates visual sensitivity". Front Cell Neurosci. 2015; 9:424. [PubMed: 26578884]

Brecha NC, Oyster CW, Takahashi ES. Identification and characterization of tyrosine hydroxylase immunoreactive amacrine cells. Invest Ophthalmol Vis Sci. 1984; 25:66–70. [PubMed: 6142028]

Brzezinski JA, Lamba DA, Reh TA. Blimp1 controls photoreceptor versus bipolar cell fate choice during retinal development. Development. 2010; 137:619–629. [PubMed: 20110327]

Brzezinski JA, Reh TA. Photoreceptor cell fate specification in vertebrates. Development. 2015; 142:3263–3273. [PubMed: 26443631]

Brzezinski JA, Uoon Park K, Reh TA. Blimp1 (Prdm1) prevents re-specification of photoreceptors into retinal bipolar cells by restricting competence. Dev Biol. 2013; 384:194–204. [PubMed: 24125957]

Bunt J, Hasselt NE, Zwijnenburg DA, Koster J, Versteeg R, Kool M. Joint binding of OTX2 and MYC in promotor regions is associated with high gene expression in medulloblastoma. PLoS One. 2011; 6:e26058. [PubMed: 22016811]

Cepko C. Intrinsically different retinal progenitor cells produce specific types of progeny. Nat Rev Neurosci. 2014; 15:615–627. [PubMed: 25096185]

Chang JC, Meredith DM, Mayer PR, Borromeo MD, Lai HC, Ou YH, Johnson JE. Prdm13 mediates the balance of inhibitory and excitatory neurons in somatosensory circuits. Dev Cell. 2013; 25:182–195. [PubMed: 23639443]

Cherry TJ, Trimarchi JM, Stadler MB, Cepko CL. Development and diversification of retinal amacrine interneurons at single cell resolution. Proc Natl Acad Sci U S A. 2009; 106:9495–9500. [PubMed: 19470466]

Das G, Choi Y, Sicinski P, Levine EM. Cyclin D1 fine-tunes the neurogenic output of embryonic retinal progenitor cells. Neural Dev. 2009; 4:15. [PubMed: 19416500]

de Melo J, Qiu X, Du G, Cristante L, Eisenstat DD. Dlx1, Dlx2, Pax6, Brn3b, and Chx10 homeobox gene expression defines the retinal ganglion and inner nuclear layers of the developing and adult mouse retina. J Comp Neurol. 2003; 461:187–204. [PubMed: 12724837]

Elshatory Y, Everhart D, Deng M, Xie X, Barlow RB, Gan L. Islet-1 Controls the Differentiation of Retinal Bipolar and Cholinergic Amacrine Cells. J Neurosci. 2007; 27:12707–12720. [PubMed: 18003851]

Euler T, Haverkamp S, Schubert T, Baden T. Retinal bipolar cells: elementary building blocks of vision. Nat Rev Neurosci. 2014; 15:507–519. [PubMed: 25158357]

Feng L, Xie X, Joshi PS, Yang Z, Shibasaki K, Chow RL, Gan L. Requirement for Bhlhb5 in the specification of amacrine and cone bipolar subtypes in mouse retina. Development. 2006; 133:4815–4825. [PubMed: 17092954]

Fossat N, Le Greneur C, Beby F, Vincent S, Godement P, Chatelain G, Lamonerie T. A new GFP-tagged line reveals unexpected Otx2 protein localization in retinal photoreceptors. BMC Dev Biol. 2007; 7:122. [PubMed: 17980036]

Fujitani Y, Fujitani S, Luo H, Qiu F, Burlison J, Long Q, Kawaguchi Y, Edlund H, MacDonald RJ, Furukawa T, Fujikado T, Magnuson MA, Xiang M, Wright CVE. Ptf1a determines horizontal and amacrine cell fates during mouse retinal development. Development. 2006; 133:4439–4450. [PubMed: 17075007]

Hanotel J, Bessodes N, Thelie A, Hedderich M, Parain K, Van Driessche B, de Brandao KO, Kricha S, Jorgensen MC, Grapin-Botton A, Serup P, Van Lint C, Perron M, Pieler T, Henningfeld KA, Bellefroid EJ. The Prdm13 histone methyltransferase encoding gene is a Ptf1a-Rbpj downstream target that suppresses glutamatergic and promotes GABAergic neuronal fate in the dorsal neural tube. Dev Biol. 2014; 386:340–357. [PubMed: 24370451]

Haverkamp S, Wassle H. Immunocytochemical analysis of the mouse retina. J Comp Neurol. 2000; 424:1–23. [PubMed: 10888735]

Haverkamp S, Wassle H. Characterization of an amacrine cell type of the mammalian retina immunoreactive for vesicular glutamate transporter 3. J Comp Neurol. 2004; 468:251–263. [PubMed: 14648683]

Hori K, Cholewa-Waclaw J, Nakada Y, Glasgow SM, Masui T, Henke RM, Wildner H, Martarelli B, Beres TM, Epstein JA, Magnuson MA, Macdonald RJ, Birchmeier C, Johnson JE. A nonclassical bHLH Rbpj transcription factor complex is required for specification of GABAergic neurons independent of Notch signaling. Genes Dev. 2008; 22:166–178. [PubMed: 18198335]

Huang L, Hu F, Feng L, Luo XJ, Liang G, Zeng XY, Yi JL, Gan L. Bhlhb5 is required for the subtype development of retinal amacrine and bipolar cells in mice. Dev Dyn. 2014; 243:279–289. [PubMed: 24123365]

Jeon CJ, Strettoi E, Masland RH. The major cell populations of the mouse retina. J Neurosci. 1998; 18:8936–8946. [PubMed: 9786999]

Jin K, Jiang H, Mo Z, Xiang M. Early B-cell factors are required for specifying multiple retinal cell types and subtypes from postmitotic precursors. J Neurosci. 2010; 30:11902–11916. [PubMed: 20826655]

Jin K, Jiang H, Xiao D, Zou M, Zhu J, Xiang M. Tfap2a and 2b act downstream of Ptf1a to promote amacrine cell differentiation during retinogenesis. Molecular brain. 2015; 8:28. [PubMed: 25966682]

Johnson J, Sherry DM, Liu X, Fremeau RT Jr, Seal RP, Edwards RH, Copenhagen DR. Vesicular glutamate transporter 3 expression identifies glutamatergic amacrine cells in the rodent retina. J Comp Neurol. 2004; 477:386–398. [PubMed: 15329888]

Kay JN, Voinescu PE, Chu MW, Sanes JR. Neurod6 expression defines new retinal amacrine cell subtypes and regulates their fate. Nat Neurosci. 2011; 14:965–972. [PubMed: 21743471]

Kondo H, Kuramoto H, Wainer BH, Yanaihara N. Discrete distribution of cholinergic and vasoactive intestinal polypeptidergic amacrine cells in the rat retina. Neurosci Lett. 1985; 54:213–218. [PubMed: 3887225]

Lee ES, Lee JY, Jeon CJ. Types and density of calretinin-containing retinal ganglion cells in mouse. Neuroscience research. 2010; 66:141–150. [PubMed: 19895859]

Li S, Mo Z, Yang X, Price SM, Shen MM, Xiang M. Foxn4 controls the genesis of amacrine and horizontal cells by retinal progenitors. Neuron. 2004; 43:795–807. [PubMed: 15363391]

Liu H, Kim SY, Fu Y, Wu X, Ng L, Swaroop A, Forrest D. An isoform of retinoid-related orphan receptor beta directs differentiation of retinal amacrine and horizontal interneurons. Nature communications. 2013; 4:1813.

MacNeil MA, Heussy JK, Dacheux RF, Raviola E, Masland RH. The shapes and numbers of amacrine cells: matching of photofilled with Golgi-stained cells in the rabbit retina and comparison with other mammalian species. J Comp Neurol. 1999; 413:305–326. [PubMed: 10524341]

MacNeil MA, Masland RH. Extreme diversity among amacrine cells: implications for function. Neuron. 1998; 20:971–982. [PubMed: 9620701]

Macosko EZ, Basu A, Satija R, Nemesh J, Shekhar K, Goldman M, Tirosh I, Bialas AR, Kamitaki N, Martersteck EM, Trombetta JJ, Weitz DA, Sanes JR, Shalek AK, Regev A, McCarroll SA. Highly Parallel Genome-wide Expression Profiling of Individual Cells Using Nanoliter Droplets. Cell. 2015; 161:1202–1214. [PubMed: 26000488]

Manes G, Joly W, Guignard T, Smirnov V, Berthemy S, Bocquet B, Audo I, Zeitz C, Sahel J, Cazevieille C, Senechal A, Deleuze JF, Blanche-Koch H, Boland A, Carroll P, Genevieve D, Zanlonghi X, Arndt C, Hamel CP, Defoort-Dhellemmes S, Meunier I. A novel duplication of PRMD13 causes North Carolina macular dystrophy: overexpression of PRDM13 orthologue in drosophila eye reproduces the human phenotype. Hum Mol Genet. 2017

Masland RH. Neuronal diversity in the retina. Curr Opin Neurobiol. 2001; 11:431–436. [PubMed: 11502388]

Menger N, Pow DV, Wassle H. Glycinergic amacrine cells of the rat retina. J Comp Neurol. 1998; 401:34–46. [PubMed: 9802699]

Mills TS, Eliseeva T, Bersie SM, Randazzo G, Nahreini J, Park KU, Brzezinski JAt. Combinatorial regulation of a Blimp1 (Prdm1) enhancer in the mouse retina. PLoS One. 2017; 12:e0176905. [PubMed: 28829770]

Mona B, Uruena A, Kollipara RK, Ma Z, Borromeo MD, Chang JC, Johnson JE. Repression by PRDM13 is critical for generating precision in neuronal identity. Elife. 2017:6.

Muranishi Y, Terada K, Inoue T, Katoh K, Tsujii T, Sanuki R, Kurokawa D, Aizawa S, Tamaki Y, Furukawa T. An essential role for RAX homeoprotein and NOTCH-HES signaling in Otx2 expression in embryonic retinal photoreceptor cell fate determination. J Neurosci. 2011; 31:16792–16807. [PubMed: 22090505]

Nishida A, Furukawa A, Koike C, Tano Y, Aizawa S, Matsuo I, Furukawa T. Otx2 homeobox gene controls retinal photoreceptor cell fate and pineal gland development. Nat Neurosci. 2003; 6:1255–1263. [PubMed: 14625556]

Park KU, Randazzo G, Jones KL, Brzezinski JAt. Gsg1, Trnp1, and Tmem215 Mark Subpopulations of Bipolar Interneurons in the Mouse Retina. Invest Ophthalmol Vis Sci. 2017; 58:1137–1150. [PubMed: 28199486]

Peichl L, Gonzalez-Soriano J. Morphological types of horizontal cell in rodent retinae: a comparison of rat, mouse, gerbil, and guinea pig. Vis Neurosci. 1994; 11:501–517. [PubMed: 8038125]

Pequignot MO, Provost AC, Salle S, Taupin P, Sainton KM, Marchant D, Martinou JC, Ameisen JC, Jais JP, Abitbol M. Major role of BAX in apoptosis during retinal development and in establishment of a functional postnatal retina. Dev Dyn. 2003; 228:231–238. [PubMed: 14517994]

Pow DV, Hendrickson AE. Distribution of the glycine transporter glyt-1 in mammalian and nonmammalian retinae. Vis Neurosci. 1999; 16:231–239. [PubMed: 10367958]

Sanes JR, Masland RH. The Types of Retinal Ganglion Cells: Current Status and Implications for Neuronal Classification. Annu Rev Neurosci. 2015; 38:221–246. [PubMed: 25897874]

Small KW, DeLuca AP, Whitmore SS, Rosenberg T, Silva-Garcia R, Udar N, Puech B, Garcia CA, Rice TA, Fishman GA, Heon E, Folk JC, Streb LM, Haas CM, Wiley LA, Scheetz TE, Fingert JH, Mullins RF, Tucker BA, Stone EM. North Carolina Macular Dystrophy Is Caused by Dysregulation of the Retinal Transcription Factor PRDM13. Ophthalmology. 2016; 123:9–18. [PubMed: 26507665]

Strettoi E, Volpini M. Retinal organization in the bcl-2-overexpressing transgenic mouse. J Comp Neurol. 2002; 446:1–10. [PubMed: 11920715]

Sugita Y, Watanabe S, Furukawa T. Response: Commentary: “Prdm13 regulates subtype specification of retinal amacrine interneurons and modulates visual sensitivity”. Front Cell Neurosci. 2015; 9:520. [PubMed: 26858608]

Surzenko N, Crowl T, Bachleda A, Langer L, Pevny L. SOX2 maintains the quiescent progenitor cell state of postnatal retinal Muller glia. Development. 2013; 140:1445–1456. [PubMed: 23462474]

Taranova OV, Magness ST, Fagan BM, Wu Y, Surzenko N, Hutton SR, Pevny LH. SOX2 is a dose-dependent regulator of retinal neural progenitor competence. Genes Dev. 2006; 20:1187–1202. [PubMed: 16651659]

Turner DL, Cepko CL. A common progenitor for neurons and glia persists in rat retina late in development. Nature. 1987; 328:131–136. [PubMed: 3600789]

Turner DL, Snyder EY, Cepko CL. Lineage-independent determination of cell type in the embryonic mouse retina. Neuron. 1990; 4:833–845. [PubMed: 2163263]

Vaney D. The mosaic of amacrine cells in the mammalian retina. Progress in Retinal Research. 1990; 9:49–100.

Voigt T. Cholinergic amacrine cells in the rat retina. J Comp Neurol. 1986; 248:19–35. [PubMed: 2424943]

Voinescu PE, Kay JN, Sanes JR. Birthdays of retinal amacrine cell subtypes are systematically related to their molecular identity and soma position. J Comp Neurol. 2009; 517:737–750. [PubMed: 19827163]

Voyvodic JT, Burne JF, Raff MC. Quantification of normal cell death in the rat retina: implications for clone composition in cell lineage analysis. Eur J Neurosci. 1995; 7:2469–2478. [PubMed: 8845952]

Watanabe S, Sanuki R, Sugita Y, Imai W, Yamazaki R, Kozuka T, Ohsuga M, Furukawa T. Prdm13 regulates subtype specification of retinal amacrine interneurons and modulates visual sensitivity. J Neurosci. 2015; 35:8004–8020. [PubMed: 25995483]

Wilken MS, Brzezinski JA, La Torre A, Siebenthall K, Thurman R, Sabo P, Sandstrom RS, Vierstra J, Canfield TK, Hansen RS, Bender MA, Stamatoyannopoulos J, Reh TA. DNase I hypersensitivity analysis of the mouse brain and retina identifies region-specific regulatory elements. Epigenetics Chromatin. 2015; 8:8. [PubMed: 25972927]

Xiang M, Zhou L, Macke JP, Yoshioka T, Hendry SH, Eddy RL, Shows TB, Nathans J. The Brn-3 family of POU-domain factors: primary structure, binding specificity, and expression in subsets of retinal ganglion cells and somatosensory neurons. J Neurosci. 1995; 15:4762–4785. [PubMed: 7623109]

Young RW. Cell death during differentiation of the retina in the mouse. J Comp Neurol. 1984; 229:362–373. [PubMed: 6501608]

Young RW. Cell differentiation in the retina of the mouse. Anat Rec. 1985; 212:199–205. [PubMed: 3842042]

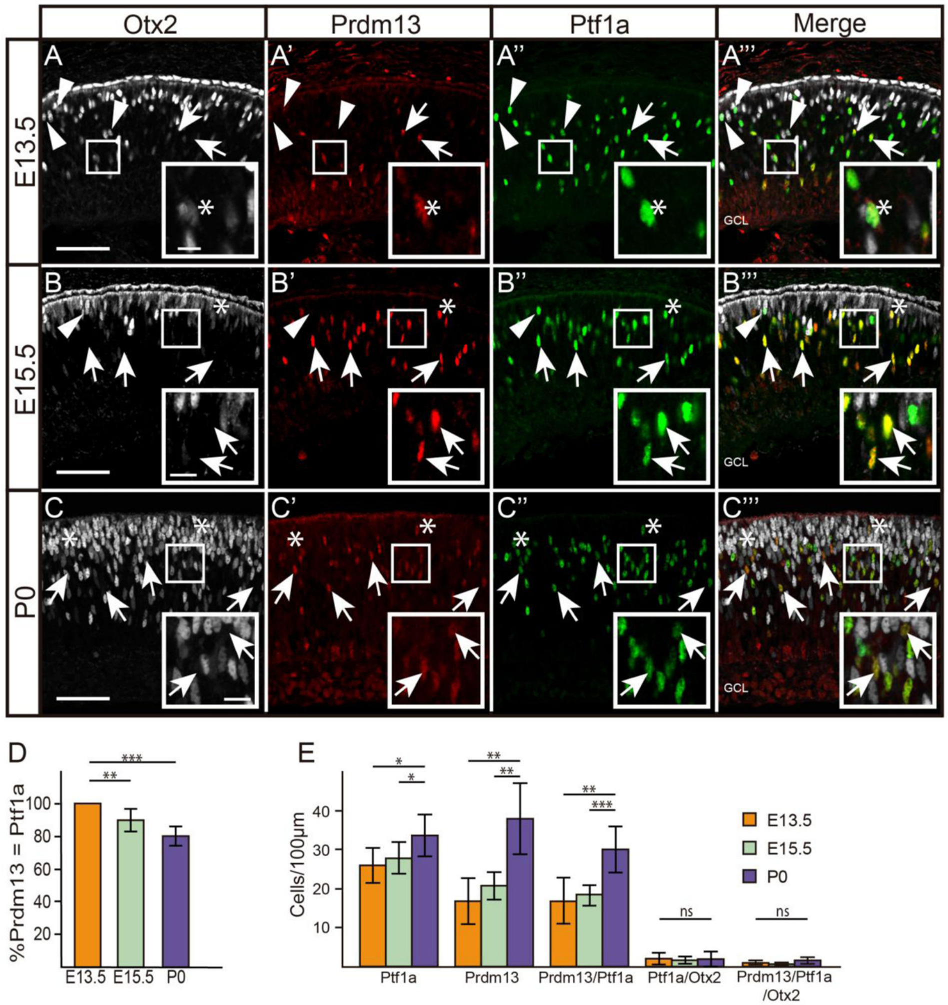

Figure 1.

Otx2, Ptf1a, and Prdm13 expression within the developing mouse retina. **(A–A‴)** Prdm13+ cells (green) in E13.5 retinas overlap with Ptf1a (red, arrows). Ptf1a/Otx2 (grey, arrowheads) and Prdm13/Ptf1a/Otx2 triple positive cells (stars) are always present in low abundance. **(B–B‴)** A similar pattern of Ptf1a, Prdm13 and Otx2 expression are seen at E15.5. **(C–C‴)** At P0, more Prdm13+ cells are evident and these overlap less frequently with Ptf1a (arrows). Ptf1a/Otx2 (arrowheads) and triple labeled cells (stars) are present. **(D)** Plot of the percentage of Prdm13+ cells that co-express Ptf1a over time. **(E)** Plot of the number of Ptf1a, Prdm13, and Otx2 labeled cells at each time-point. Sample sizes at E13.5 and E15.5 are 4 mice each and 3 mice are quantified at P0. Statistical significance determined by unpaired two-sample t-tests: * $P < 0.05$, ** $P < 0.01$, *** $P < 0.001$, Error bars represent standard deviation. Scale bar 50µm. Inset scale bar 10µm. GCL, ganglion cell layer; ns, not significant.

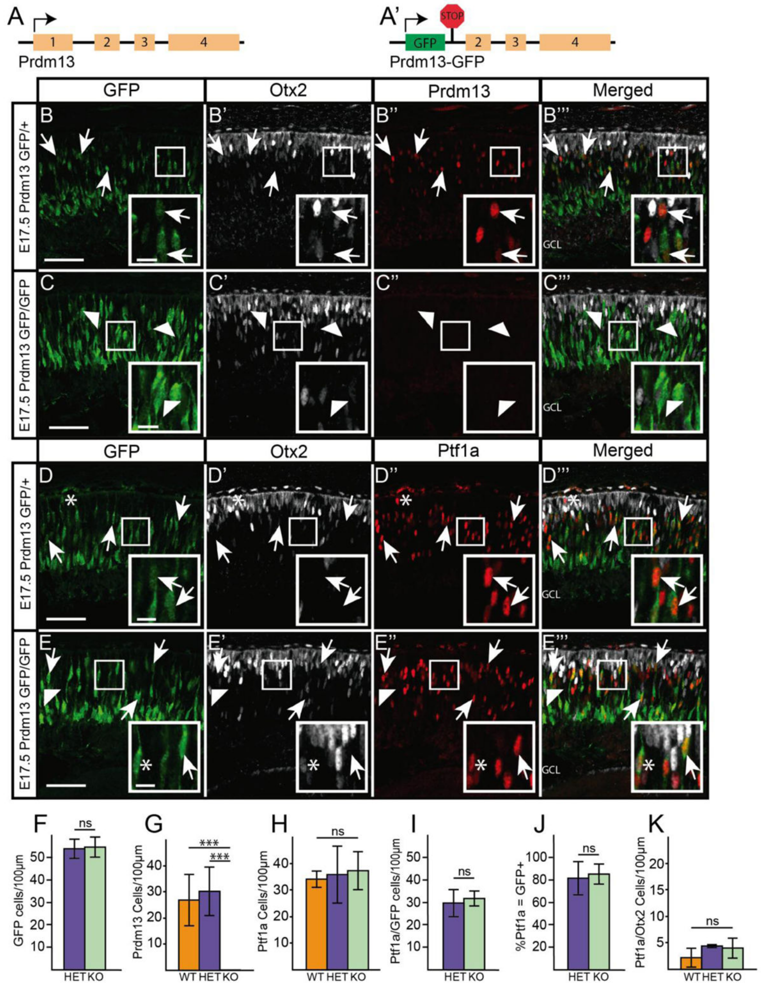

Figure 2.

Prdm13-GFP knock-in mice reveal *Prdm13* expression at E17.5. **(A–A′)** Schematic of wildtype (A) and *Prdm13-GFP* mice (A′). The first exon of *Prdm13* is replaced with GFP followed by a stop codon. Note that all homozygous *Prdm13-GFP/GFP* null mice die by birth. **(B–B‴)** All Prdm13+ (red) cells co-express GFP (green, arrows) in E17.5 *GFP/+* mice. However, some GFP+ cells do not express Prdm13, likely because of the long half-life of GFP. **(C–C‴)** Homozygous *GFP/GFP* mutants have a similar number of GFP+ cells compared to heterozygous controls, but lack Prdm13+ cells. A subset of Prdm13-GFP+ cells co-express Otx2 (grey, arrowheads). **(D–E‴)** Heterozygous control (D) and mutant (E) retinas stained for GFP (green), Otx2 (grey), and Ptf1a (red). The Ptf1a and Otx2 staining patterns are equivalent between genotypes. Arrows mark Ptf1a+/GFP+ cells, arrowheads mark Otx2+/GFP+ cells, and stars mark triple labeled cells. **(F–G)** Plots showing GFP+ cells in heterozygotes (HET) and *GFP/GFP* knock-outs (KO) (F), and Prdm13+ cells in WT, HET and KO animals (G). **(H–K)** Plots of the number of Ptf1a+ cells (H), Ptf1a/GFP double labeled cells (I), percentage of Ptf1a that express GFP (J), and the number of Ptf1a+/Otx2+ cells (K). Sample sizes are 3–4 mice per condition. Statistical significance determined by unpaired two-sample t-tests and 1-way ANOVA: * $P < 0.05$, ** $P < 0.01$, *** $P < 0.001$. Error bars represent standard deviation. Scale bar 50μm. Inset scale bar 10 μm.

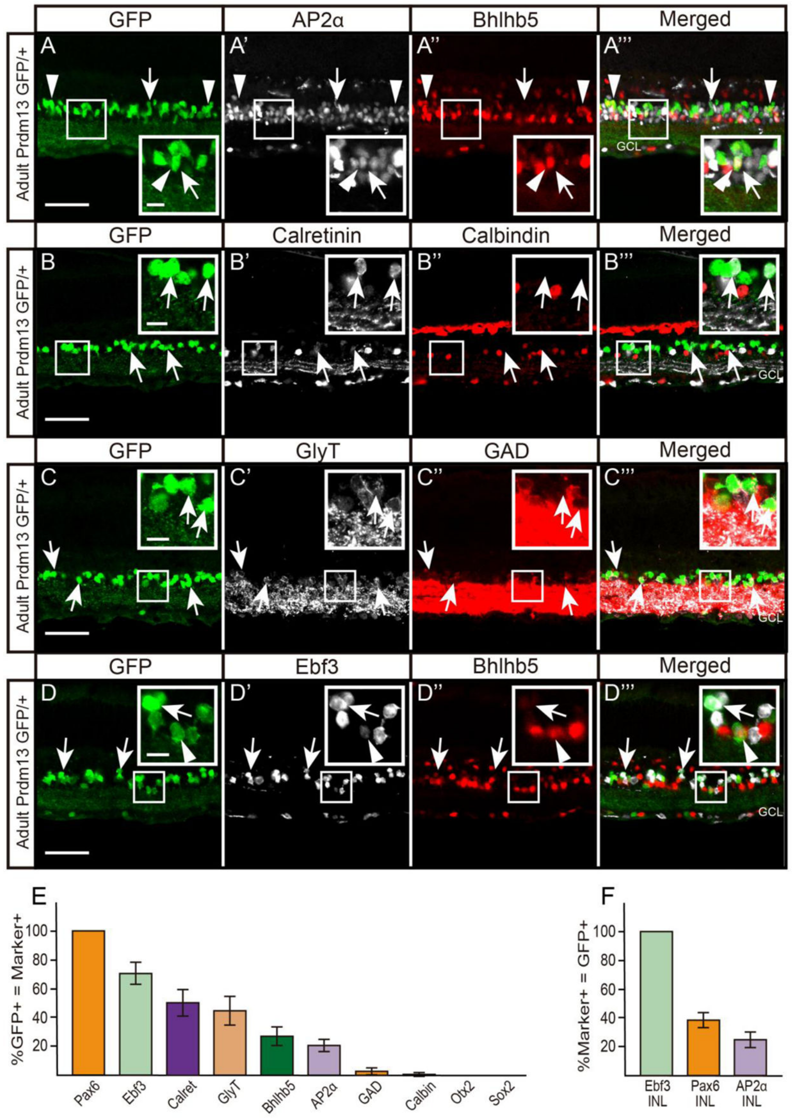

Figure 3.

Prdm13 marks a subset of amacrines in the adult retina. **(A–D‴)** P30 Prdm13-GFP/+ heterozygous animals co-stained with GFP (green) and amacrine cell markers (grey/red). **(A–A‴)** A small subset of Prdm13-GFP+ amacrine cells co-express AP2α (grey, arrows) and Bhlhb5 (red, arrowheads). **(B–B‴)** Nearly half of GFP+ cells co-express calretinin (grey, arrows), while less than 1% of GFP+ cells co-express calbindin (red). No intensely calretinin+ horizontal cells co-express GFP. **(C–C‴)** A large fraction of GFP+ cells co-express the glycinergic amacrine marker GlyT (grey, arrows), but few GFP+ cells co-express the GABAergic marker GAD65/67 and these were sometimes GlyT+ as well. **(D–D‴)** The majority of GFP+ cells co-express Ebf3 (grey, arrows), but all Ebf3+ cells in the INL are GFP+. A minority of GFP+ cells co-express Bhlhb5 (red, arrowheads) and cells that co-express Bhlhb5, Ebf3, and GFP are rarely seen. **(E)** Plot of the percentage of GFP+ cells that co-express a given marker. GFP does not overlap with Brn3, TH, or vGlut3 (not shown). **(F)** Plot showing the percentage of Ebf3+ amacrines, Pax6+ INL nuclei, and AP2α+ INL cells that co-express Prdm13-GFP. Sample size was 3 mice per condition. Statistical significance determined by unpaired two-sample t tests: * $P < 0.05$, ** $P < 0.01$, *** $P < 0.001$. Error bars represent standard deviation. Scale bar 50μm. Inset scale bar 10μm. INL, inner nuclear layer.

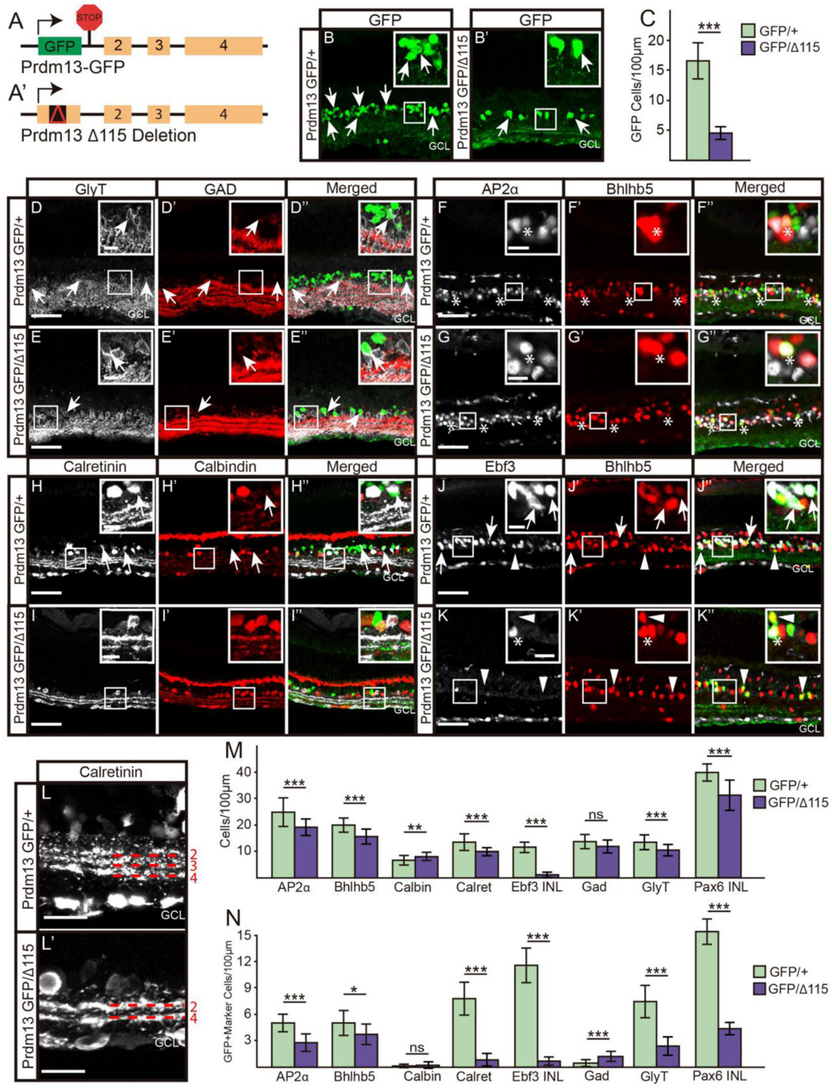

Figure 4.

Ebf3+ amacrines are lost in adult *Prdm13* mutants. **(A–A′)** Schematics of the two transgenic mice, *Prdm13-GFP* (A) and *Prdm13-Δ115* (A′). The *Δ115* allele has an 115bp deletion in the first exon of *Prdm13*. Unlike homozygous *Prdm13-GFP* mice, homozygous *Δ115/Δ115* mice and compound heterozygous *Prdm13-GFP*/*Δ115* are viable. **(B–B′)** *Prdm13-GFP/Δ115* mice (B′) have far fewer GFP+ cells (arrows) than *Prdm13-GFP/+* control mice (B). **(C)** Plot showing the reduction in GFP+ cells between the two genotypes. **(D–K)** *Prdm13-GFP/+* and *Prdm13-GFP/Δ115* retinas stained for GFP (green) and various amacrine cell markers (red, grey). **(D–E″)** The number of GlyT (grey) and GAD+ (red) cells is modestly altered in *Prdm13-GFP/Δ115* mice (E) versus controls (D). The number of GlyT+/GFP+ cells (arrows) is reduced in *Prdm13-GFP/Δ115* mice. **(F–G″)** Staining for AP2α (grey) and Bhlhb5 (red) show a small decrease in both populations in *Prdm13-GFP/Δ115* mice (E) compared to controls (F). Cells expressing GFP, AP2α, and Bhlhb5 are marked by stars. **(H–I″)** Calbindin (red) staining is similar between genotypes and rarely overlaps with GFP, but calretinin (grey) stains revealed a disrupted IPL in *Prdm13-GFP/Δ115* mice. There are fewer calretinin+ cells in the INL and far fewer GFP+/calretinin+ cells in *Prdm13-GFP/Δ115* mice compared to *Prdm13-GFP* controls (arrows). **(J–K″)** Ebf3+ (grey) amacrine cells are almost entirely absent from the INL in *Prdm13-GFP/Δ115* mice. GFP+/Ebf3+ cells (arrows) are rare in *Prdm13-GFP/Δ115* mice (K) compared to control (J). Some Bhlhb5+/GFP+ cells are seen in both conditions, some of which are Ebf3+/Bhlhb5+/GFP+ (stars). **(L–L′)** Close up views of calretinin staining in control (L) and *Prdm13-GFP/Δ115* (L′) retinas. Loss of sublamina 3 and a thinning of the IPL are evident. **(M)** Plot showing the number of marker positive cells in control and *Prdm13-GFP/Δ115* mice. **(N)** Plot showing the number of marker positive cells that co-express GFP. Sample sizes are 3 mice per condition for heterozygotes and 6 mice for mutants. Statistical significance determined by unpaired two-sample t tests: * $P < 0.05$, ** $P < 0.01$, *** $P < 0.001$. Scale bar 50μm, inset scale bar 10μm, scale bar for L 20μm. Error bars represent the standard deviation.

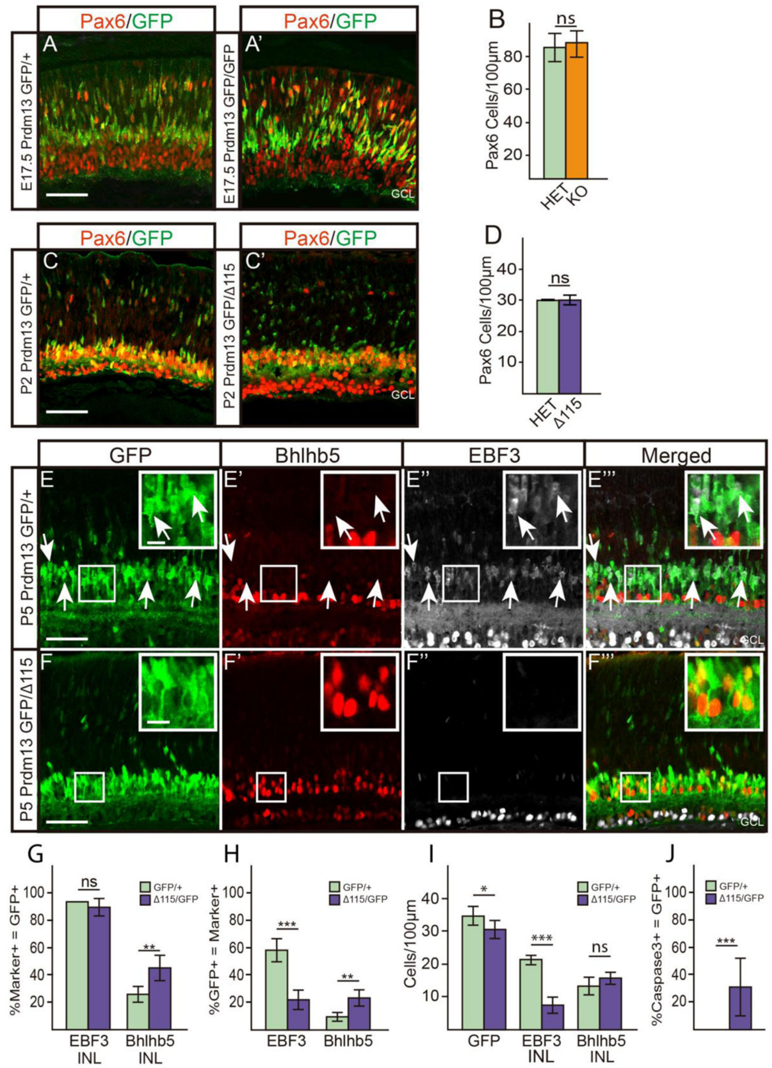

Figure 5.

Amacrine cells are initially formed, but subsets are lost in the first postnatal week of *Prdm13* mutants. **(A–B)** At E17.5, there is no difference in Pax6 (red) numbers between *Prdm13-GFP/+* control (A) and *Prdm13-GFP/GFP* null mice (A′). GFP (green) staining is equivalent between these genotypes. **(C–D)** P2 Prdm13-GFP/+ (C) and *Prdm13-GFP/Δ115* mice (C′) have equivalent GFP staining and Pax6 numbers. **(E–F‴)** P5 Prdm13-GFP/+ control (E) and Prdm13-*GFP/Δ115* (F) retinas stained for GFP (green), Bhlhb5 (red) and Ebf3 (grey). At this age, there are fewer GFP+ cells in *Prdm13-GFP/Δ115* retinas. Controls have many cells that co-express GFP and Ebf3 (arrows), but Ebf3+ cells are nearly absent from the INL of *Prdm13-GFP/Δ115* mice. A higher percentage of GFP+ cells co-express Bhlhb5 in mutants. **(G)** Plot showing the percentage of marker positive cells that co-express GFP at P5. **(H)** Plot showing the percentage of GFP+ cells that co express Ebf3 and Bhlhb5. **(I)** Plot showing the number of cells that express GFP, Ebf3, and Bhlhb5. Sample size for E17.5 is one mouse, 3 mice per condition at P2, and 3–4 mice per condition at P5. Statistical significance determined by unpaired two-sample t-tests: * $P < 0.05$, ** $P < 0.01$, *** $P < 0.001$. Error bars represent the standard deviation. Scale bar 50μm. Inset scale bar 10μm.

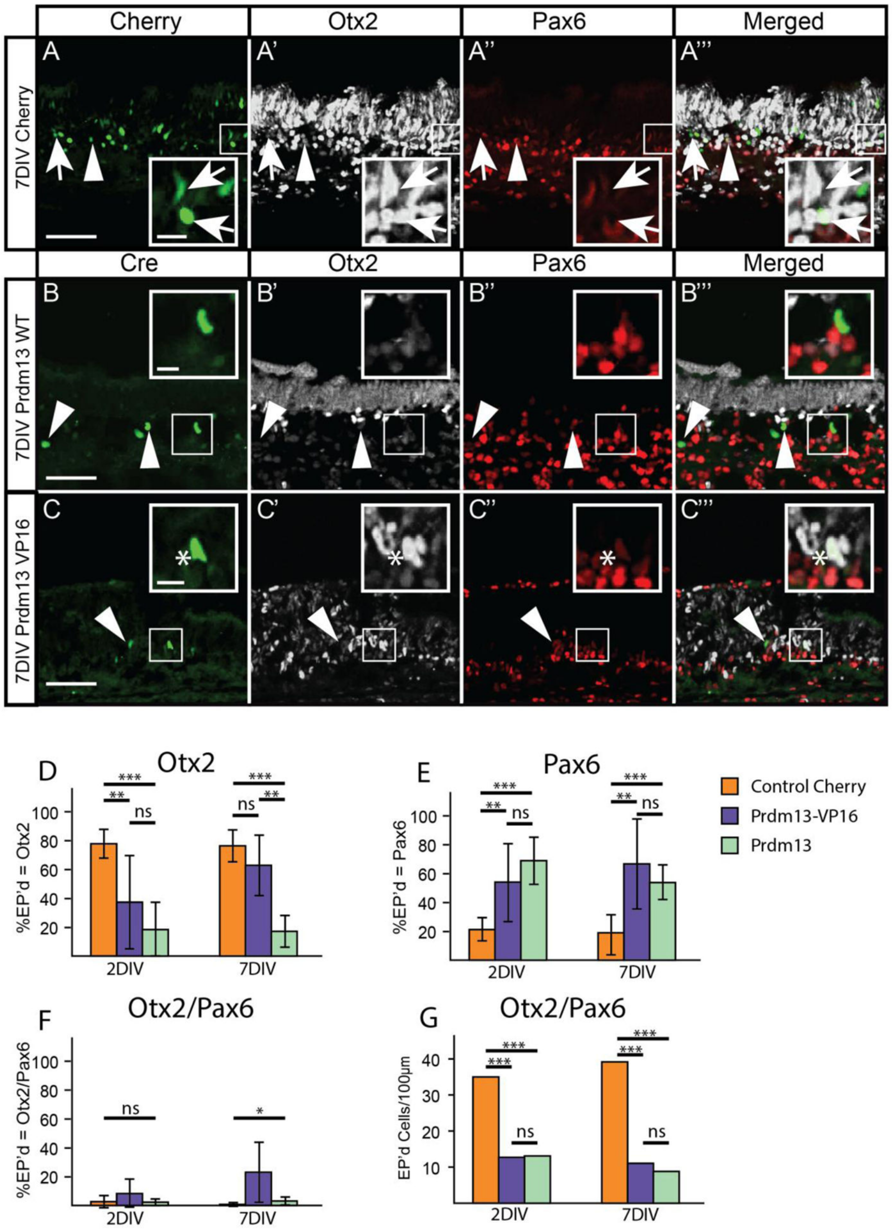

Figure 6.

Overexpression of *Prdm13* does not specify amacrine identity and is toxic to photoreceptors. **(A–C‴)** Wild-type P0 mouse retinas electroporated (EP′d) with control, wild-type Prdm13, and Prdm13-VP16 expression plasmids and cultured for 7 days *in vitro* (DIV). Electroporated cells are detected with antibodies to Cre (Prdm13 and Prdm13-VP16) or to red fluorescent protein (RFP, control). Sections are stained for the photoreceptor and bipolar cell marker Otx2 (grey) and for Pax6 (red), which marks amacrine cells intensely. **(A–A‴)** Control Ef1α nuclear Cherry transfections have numerous RFP cells (pseudo-colored green), primarily in the photoreceptor area after 7DIV. Most of these cells co-express Otx2 (arrows), while a minority co-express Pax6 (arrowheads). **(B–B‴)** Overexpression of wild-type Prdm13 (Prdm13-WT-IRES-Cre) yields few Cre+ (green) cells after 7DIV. These cells are localized to the INL and are typically Pax6+ (arrowheads). In about 30% of cases, Cre+ cells expressed neither Pax6 nor Otx2 (inset). **(C–C‴)** Electroporation of a Prdm13-VP16 fusion (Prdm13-VP16-IRES-Cre) construct also results in sparse numbers of Cre+ cells. These transfected cells are seen in the INL and co-express Pax6 (arrowheads) at high frequency. Many of these cells also co-express Otx2 (star), which is rarely seen in control or Prdm13 WT transfections. **(D–F)** Plots showing the percentage of electroporated cells at 2DIV and 7DIV that co-express Otx2 (D), Pax6 (E), and Otx2/Pax6 (F). **(G)** Plot showing the number of transfected cells seen after 2DIV or 7DIV. Sample sizes for 2DIV are 8–10 retinas per condition and for 7DIV are 7–9 retinas per condition. Statistical significance is determined by unpaired two-sample t-tests (D, E, G), and ANOVA (F): * $P < 0.05$, ** $P < 0.01$, *** $P < 0.001$. Error bars represent the standard deviation. Scale bar 50μm. Inset scale bar 10μm.